

VISIBILITY RANGE OF THE UNDERWATER OBJECTS

E.P. Zege, I.L. Katsev, and A.S. Prikhach

*B.I. Stepanov Institute of Physics
of the Belorussian Academy of Sciences, Minsk*

Received April 20, 1992

A new concept of determining the visibility range of the objects in the scattering media based on the ideas of optimum processing of image is presented. The practical realization of this concept is described in the form of the program for calculation of maximum ranges of detection and discrimination of underwater objects (including that through the water—air interface) with the help of passive television and active laser-television observational systems. The characteristic features of the program for personal computer complexes as well as of the specially-developed convenient few-parameter models of the optical characteristics of water, interface, and atmosphere implemented in the program are described. The certain examples of calculations of maximum visibility range are presented.

The general character of the concept and modularity of the program make it possible to extend substantially its capabilities.

INTRODUCTION

One of the main practical problems of the theory of vision in the scattering media is an *a priori* investigation of the possibilities of the instrumental observational systems and, in particular, estimate of maximum ranges of detection and discrimination of the objects. The present paper is devoted to a brief description of the developed concept of optimum detection and its use in the method of calculation of maximum ranges of detection and discrimination of the objects in the scattering medium including the underwater objects.

The concept of optimum detection as well as a number of problems concerning the relationship between the noise characteristics of the medium (including the wavy ocean surface) and the vision system with threshold contrast were discussed in Ref. 1. Later these results provided the basis for elaboration of engineering calculational techniques and program package for personal computers capable of calculating the maximum detection and discrimination ranges depending on the parameters of a video system and optical characteristics of water and atmosphere in the effective interactive mode.

In this paper we present the integral successive description of the problem, namely,

- on the basis of the concept of the optimum detection we formulate mathematically the problem of determining the maximum ranges of the television detection and discrimination of the objects in the scattering medium;

- we describe the simple model of the ocean—atmosphere system which meets the requirements for compromise between the number of the input system parameters and the most adequate description of the conditions of radiation propagation under different weather conditions in various zones of the seas and oceans; and,

- we present the basic formulas for calculating the signals, backgrounds, and noise, capable of achieving the compromise between the accuracy and time of calculations.

In addition, we give some examples of solving by such a method not only some classic vision problems but also new problems connected, in particular, with observations through the wavy sea surface.

1. DETECTION AND DISCRIMINATION OF OBJECTS IN THE SCATTERING MEDIUM

1.1. Visual perception of the real objects. Jonson's criterion. The modern vision theory,^{1,2} which is based on the radiative transfer theory and the theory of linear systems, enables one to determine, with one or another accuracy, practically all the parameters of the light field at the photodetector and the image quality characteristics and, in particular, to calculate the frequency-contrast characteristic of the viewing system as well as the energetics of the valid signal and noise at the photodetector. It enables one to calculate even the structure of image of any given real object. However, it is insufficient for *a priori* assessing the capabilities of the viewing system as well as for estimating the maximum range of detection of the real objects in the scattering medium. In view of the variety of the real objects and due to the specific character of their perception associated with a number of individual features of the observer, it is necessary to have the relationship between the characteristics of the video systems, when viewing the standard test objects, and the quality of vision under the real conditions. It is clear that such a relationship can have only statistical character. For one class of the objects it was obtained by Jonson.^{3,4} By the example of the troopship Jonson compared the ability of the observer to resolve the image of a mira and his ability to detect, to distinguish, and to identify the real objects. As a result, each degree of vision was related to the number of resolvable half-periods of the equivalent hatched mira on the object of minimum (critical) size (see Table I).

TABLE I. Jonson's criteria of vision quality.

Degree of vision	The number of resolvable half-periods of the hatched mira on the object of minimum size
Detection	2.0 ± 0.5
Determination of orientation	2.8 ± 0.8
Recognition (discrimination)	8.0 ± 1.6
Identification	12.8 ± 3.0

The equivalent hatched mira is taken to mean the rectangular mira, whose total width equals to the critical size of the object while the length corresponds to the size of the object in the direction normal to the critical one. It follows from the table, that the object is detected (that is, its appearance in the field of view is fixed) if two half-periods (one period) of hatched mira are resolved on the object of minimum size. Recognition (discrimination) of the object (that is, its classification, for example, as a house, a car, a man, and so on) is possible if eight half-periods of hatched mira can be resolved on the object of minimum size.

Thus, Jonson's criteria permit one to relate the quality of visual perception of the real objects by the given video system to the theoretically estimated characteristics of the image quality of the test objects. In particular, the problem of detection of the real objects reduces to the problem of detection of the test object of rectangular shape. In so doing the width of the test object is half the size of the real object, its albedo is equal to the mean albedo of the real object, while the background albedo equals to the mean albedo of the real background.^{3,4} This very test object is considered below in the problem of estimating the maximum detection range of the object. We stress once more that here the notion *detection* is taken to mean only establishing the fact of the object appearance in the field of view of the detector (possibly, in the form of a blurred spot). In this context this term differs from the notion *detection* used in the commercial (everyday) television, which is normally taken to mean the degree of vision of a higher quality (apparently, it is closer to our term *discrimination*).

1.2. Signal-to-noise ratio. Criterion of detection.

The basic characteristic of the image quality is the signal-to-noise ratio^{1,2,5}

$$\delta = \Delta N / \sqrt{\sigma_N^2} . \tag{1.1}$$

Here ΔN is the difference between the number of photons striking the test image element over the observational period and the average number $\langle N \rangle$ of photons striking the areas being of the same size and surrounding this element and σ_N^2 is the variance of the fluctuations in the number of photons N about their average value $\langle N \rangle$. Here N , $\langle N \rangle$, and ΔN are the numbers of used photons, that is, related to the corresponding numbers of photons striking the photodetector by the photodetector quantum efficiency.

Disregarding the dark-current noise of the photodetector (for television systems in the visible range it may be practically always neglected), we obtain

$$\sigma_N^2 = \langle N \rangle + \alpha \langle N \rangle^2 , \tag{1.2}$$

where the first term describes the shot noise of the photodetector, while the second refers to the intrinsic noise of the receiving system (due to the fluctuations of the gain and so on). In principle, the second term may include also the noise due to the instability of the radiation power emitted by the source, the nonuniformity of the photodetector sensitivity, the fluctuations of the optical characteristics of the medium in the image transmission channel,^{6,7} etc. For instance, in the case of viewing through the medium with the fluctuating optical parameters⁸

$$\sigma_N^2 = \langle N \rangle + [\alpha + 2K_f(1 - B_f(r_0))]\langle N \rangle^2 , \tag{1.3}$$

where K_f is the coefficient of variation of fluctuation noise of the medium, $B_f(r_0)$ is the spatial correlation function of the noise, and r_0 is the distance between the image elements

being compared. In addition, $B_f(r_0 = 0) = 1$. As $r_0 \rightarrow \infty$ the quantity $B_f(r_0) \rightarrow 0$ and

$$\sigma_N^2 = \langle N \rangle + (\alpha + 2K_f)\langle N \rangle^2 . \tag{1.4}$$

If the distance r_0 between the compared elements is much less than the correlation length for the noise of the medium, then $B_f(r_0) = 1$ and

$$\sigma_N^2 = \langle N \rangle + \alpha \langle N \rangle^2 , \tag{1.5}$$

that is, in this case the noise variance σ_N^2 and hence the signal-to-noise ratio are independent of the fluctuations in the optical parameters of the medium.

Such a situation can take place, for example, in viewing through the wavy sea surface, when the long-period swell, whose scale is comparable or exceeds the frame size, does not practically distort the object image and causes only its slow swinging.

The parameter α is the parameter of the video system itself and, as can be seen from Eqs. (1.1) and (1.2), without fluctuations of the characteristics of the medium in the image transfer channel this parameter relates the threshold value of the signal-to-noise ratio δ_{th} to the threshold contrast k_{th} of the system for optimum, i.e., sufficiently strong illumination ($\alpha \langle N \rangle \gg 1$).⁴ Indeed, in this case

$$\delta = \frac{1}{\sqrt{\alpha}} \frac{\Delta N}{\langle N \rangle} = \frac{1}{\sqrt{\alpha}} k , \quad k = \frac{\Delta N}{\langle N \rangle} \tag{1.6}$$

and

$$\delta_{th} = k_{th} / \sqrt{\alpha} , \quad k_{th} = \delta_{th} \sqrt{\alpha} . \tag{1.7}$$

Relation (1.7) defining k_{th} in terms of δ_{th} , can be regarded also as the definition of the parameter α in terms of the threshold quantities δ_{th} and k_{th} .

The threshold quantity δ_{th} , generally speaking, is not a fixed characteristic of the video system but depends on the requirements imposed on the system when solving one or another specific problem. As is well known, this quantity is determined in terms of the permissible values of the probability of erroneous alarm P_{er} and the detection probability P_{det} . For $\Delta N \ll \langle N \rangle$ the quantity $\delta_{th} = \delta^*$ is the solution of the system of equations^{9,10}

$$\begin{cases} P_{er} = (1/2) \operatorname{erfc} y / \sqrt{2} , \\ P_{det} = (1/2) \operatorname{erfc} (y - \delta^*) / \sqrt{2} , \end{cases} \tag{1.8}$$

where

$$\operatorname{erfc} z = 1 - (2/\sqrt{\pi}) \int_0^z \exp(-t^2) dt .$$

It can be shown that for arbitrary relation between ΔN and $\langle N \rangle$, the formula for the threshold signal-to-noise ratio has the form

$$\delta_{th} = \delta^* + (\delta^* - y) \left[\frac{\sqrt{\sigma_{N+\Delta N}^2}}{\sqrt{\sigma_N^2 - 1}} \right] . \tag{1.9}$$

If $\Delta N \ll \langle N \rangle$ this relation transforms into Eq. (1.8). Thus, the only criterion responsible for the object visibility is the condition

$$\delta \geq \delta_{th} ,$$

where δ_{th} is given by formula (1.8). It should be noted that when this condition is satisfied, the condition $k \geq k_{th}$ and the requirement for the minimum signal energy at the input of the photodetector, associated with its threshold sensitivity, are always satisfied as well.

1.3. Optimum detector. Detection range. In the problem of television or visual viewing of the object in the scattering medium the energies of the signals being fed to two image elements are compared (for example, in the problem of detection of the object one of them corresponds to the center of object, while another determines the level of the background). For this reason in formulas (1.1) and (1.2) we assume

$$\Delta N = CW_{vs} , \quad \langle N \rangle = CW_{bg} , \tag{1.10}$$

where W_{vs} is the energy of the valid signal, i.e., the difference between the energies acquired by two compared image elements; W_{bg} is the background energy acquired by the image element over the period of frame recording. The proportionality factor C is determined by the photodetector quantum efficiency $\eta = C\omega_0$, where $\omega_0 = h\nu$ is the energy of a single photon. If the value of η is well known for the system, then $C = \eta/\omega_0$.

By substituting Eq. (1.10) into Eq. (1.1) and taking Eq. (1.2) into account, we have

$$\delta = \frac{W_{vs}}{\sqrt{W_{bg}/C + \alpha W_{bg}^2}} . \tag{1.11}$$

Formula (1.11) can be used to calculate the signal-to-noise ratio for the prescribed conditions of observation and the system parameters. One of these parameters determining the value of δ is the area Σ_{el} of the image element over which the signal is integrated.

The minimum possible area of the element Σ_{el} is determined by the parameters of the viewing system (by the field of view of the television frame and the number of elements in it, by the area of receptor of the viewing system, etc.). However, the element size can be increased by spatial integration of the image that has been already formed. Therefore, when estimating the maximum detection range of the objects, it is necessary to solve the problem of optimization, i.e., to implement such a procedure for image processing, for which the value of δ and accordingly the detection range are maximum.

For small Σ_{el} , apparently, $W_{vs} \sim \Sigma_{el}$, $W_{bg} \sim \Sigma_{el}$, and $\delta \sim \sqrt{\Sigma_{el}}$. When the element area is sufficiently large and comparable to the area of the object image, with increase of Σ_{el} the value of W_{vs} is saturated, while δ decreases. Therefore, it can be accepted that the signal-to-noise ratio δ attains its maximum at certain optimum value $\Sigma_{el} = \Sigma_{el}^{opt}$. Choosing the value of Σ_{el} in such a manner we can obviously achieve the maximum reliability of the decision about the presence of the object in the medium. Such a processing is analogous to the construction of the optimum filter, i.e., as a matter of fact similar to optimizing against the well-known Neumann-Pearson and Siebert-Kotel'nikov criteria.¹¹

Such an image processing, i.e., selection of optimum element Σ_{el}^{opt} and corresponding integration of signal is performed by the sight organs of a man (an eye plus a brain) both under the normal conditions of visual observations and when watching the television image. This statement was experimentally confirmed in Ref. 12.

For observations in the scattering medium the quantity Σ_{el}^{opt} is a function of the distance L to the object. For this reason, the problem of finding the maximum detection range L_{det} consists in searching for the conditions under which $\Sigma_{el} = \Sigma_{el}^{opt}$ and $\delta = \delta_{th}$ simultaneously, i.e., reduces to the solution of the system of equations

$$\begin{cases} d\delta(L, \Sigma_{el})/d\Sigma_{el} = 0 , \\ \delta(L, \Sigma_{el}) = \delta_{th} . \end{cases} \tag{1.12}$$

The background energy W_{bg} acquired by the image element in general may be represented by the sum of the backscatter interference energy W_{bs} and the energy of external (solar) illumination W_{il} . The formulas for calculation of these quantities are presented in Sec. 4.1. Here it is important for us to stress that $W_{bg} = W'_{bg\Sigma_{el}}$ or for Jonson's test object of a rectangular shape

$$W_{bg} = W'_{bg} d_{xel} d_{yel} , \tag{1.13}$$

where W'_{bg} is the background energy density per unit area of the object independent of d_{xel} and d_{yel} . Here and below the quantities d_{xel} and d_{yel} represent the linear dimensions of the element of spatial integration along the x axis (the direction of critical size of the object) and the y axis in the object plane.

The energy of the valid signal W_{vs} can be expressed in the form

$$W_{vs} = W\eta_{vs} |A_{ob} - A_{bg}| \Psi_1 , \tag{1.14}$$

where W is the energy of the radiation source over the period of frame recording, η_{vs} is the transmission coefficient of the valid signal when viewing the uniform surface with albedo $A(\mathbf{r}) = 1$ (\mathbf{r} is the coordinate in the object plane) and A_{ob} is the mean albedo of the object. The difference $A_{ob} - A_{bg}$ takes into account shading of the region of the medium lying behind the object, where A_{bg} is the albedo of the layer of the medium lying behind the object. The function Ψ_1 (see Sec. 4.2) describes the dependence of the energy W_{vs} on the size and shape of the object and on the dimensions of the element of integration d_{xel} and d_{yel} .

The transmission coefficient η_{vs} can be written in the form

$$\eta_{vs} = \eta'_{vs} d_{xel} d_{yel} , \tag{1.15}$$

where η'_{vs} is independent of d_{xel} and d_{yel} . Substituting Eqs. (1.13), (1.14), and (1.15) into Eqs. (1.11) and (1.12) we obtain the system of three equations

$$\frac{\partial \ln \delta(L, d_{xel}, d_{yel})}{\partial d_{xel}} = \frac{\partial \ln \Psi_1}{\partial d_{xel}} + \frac{1}{2d_{xel}} \cdot \frac{1}{1 + 2CW_{bg}} = 0 ,$$

$$\frac{\partial \ln \delta(L, d_{x\text{el}}, d_{y\text{el}})}{\partial d_{y\text{el}}} = \frac{\partial \ln \Psi_1}{\partial d_{y\text{el}}} + \frac{1}{2d_{y\text{el}}} \cdot \frac{1}{1 + 2CW_{\text{bg}}} = 0, \quad (1.16)$$

$$\delta(L, d_{x\text{el}}, d_{y\text{el}}) = \delta_{\text{th}}.$$

The solution of this system on account of Eq. (1.11) determines the dimensions $d_{x\text{el}}^{\text{opt}}$ and $d_{y\text{el}}^{\text{opt}}$ of the optimum element of spatial integration along two axes and the maximum detection range of the object L_{det}^* .

1.4. Discrimination of the object. In this case in accordance with Jonson's criteria it is necessary to resolve eight half-periods of hatched mira on the object of critical size (we assume conventionally that the critical direction coincides with the x axis, while the object critical size is equal to $d_{x\text{ob}}$). This apparently imposes limitations on the size of the element of integration of the image along the x axis in the form of the condition $d_{x\text{el}} \leq d_{x\text{ob}}/8$. However, as the estimates and numerical calculations show, practically for all situations of interest arising in the problem of object detection $d_{x\text{el}}^{\text{opt}} > d_{x\text{ob}}/8$. Therefore, below in the calculation of the maximum object discrimination range the value of $\Sigma_{\text{el}}^{\text{opt}}$ is assumed to be fixed and equal to

$$\Sigma_{\text{el}} = d_{x\text{el}} d_{y\text{el}} \quad (1.17)$$

for

$$d_{x\text{el}} = d_{x\text{ob}}/8, \quad d_{y\text{el}} = \min\{d_{y\text{ob}}, d_f\},$$

where $d_{y\text{ob}}$ is the object size along the y axis and d_f is the frame size.

Thus, the search for the maximum range of object discrimination L_{dis}^* reduces approximately to the solution of the equation

$$\delta(L, d_{x\text{el}}^{\text{opt}}, d_{y\text{el}}^{\text{opt}}) = \delta_{\text{th}} \quad (1.18)$$

taking Eqs. (1.11) and (1.17) into account.

2. OPTICAL MODEL OF THE OCEAN-ATMOSPHERE SYSTEM

The following model of the ocean-atmosphere system is considered in the paper: the plane-parallel comparatively thin layer (atmosphere) adjoining the semi-infinite medium (ocean) with refracting and reflecting interface (refractive index at the interface $n = 1.34$). The effect of the interface (refraction, reflection, and transmission) is taken into account based on the Fresnel formulas.

2.1. The ocean. Let us restrict ourselves to the model of a uniform layer of sea water whose optical properties are assigned by the extinction coefficient ϵ , the photon survival probability Λ , and the scattering phase function $x(\beta)$ (β is the scattering angle). It is assumed that the function $x(\beta)$ is normalized as follows:

$$\frac{1}{2} \int x(\beta) \sin \beta \, d\beta = 1. \quad (2.1)$$

In addition, we introduce the absorption coefficient κ and the scattering coefficient σ with $\epsilon = \kappa + \sigma$ and $\Lambda = \sigma/\epsilon$. For prognostic and methodical investigations it is useful to have the few-parameter model of the optical properties of the ocean with analytically assigned scattering phase function. Such a problem can be solved leaning upon the

well-known model^{13,14} of sea water consisting of the coarse organic and fine terrigenous fractions of suspension, pure water, and dissolved yellow matter.

Scattering phase function. The scattering phase function for each sea water component, normalized according to Eq. (2.1), is

$$x_i(\beta) = \sigma_i(\beta)/\sigma_i, \quad (2.2)$$

where $\sigma_i(\beta)$ is the absolute brightness phase function for the i th component, while

$$\sigma_i = (1/2) \int \sigma_i(\beta) \sin \beta \, d\beta. \quad (2.3)$$

If the concentrations of coarse and fine fractions of suspension observed in the given region are C_c and C_f , respectively, then the scattering coefficient and scattering phase function of water can be calculated with the use of formulas

$$\sigma = \sigma_w + C_c \sigma_c^0 + C_f \sigma_f^0, \quad (2.4)$$

$$x(\beta) = \frac{\sigma_w x_w(\beta) + C_c \sigma_c^0 x_c(\beta) + C_f \sigma_f^0 x_f(\beta)}{\sigma}, \quad (2.5)$$

where the subscript w stands for pure water, the subscripts c and f refer to coarse and fine fractions, σ_c^0 and σ_f^0 are the scattering coefficients of coarse and fine fractions of unit concentration. It is characteristic that at $\beta < 2^\circ$ the scattering phase function of the sea water is practically entirely determined by the coarse fraction, while at $\beta > 15^\circ$ — by the fine fraction, whereas scattering by water is significant only at $\beta > 90^\circ$. At $\beta > 90^\circ$ the scattering phase function varies slightly and is assumed to be isotropic. Then the scattering phase function of sea water can be prescribed by the function

$$x(\beta) = \begin{cases} F[ax_c(\beta) + (1-a)x_f(\beta)], & 0 \leq \beta \leq \pi/2, \\ 2(1-F), & \pi/2 \leq \beta \leq \pi, \end{cases} \quad (2.6)$$

where F is the fraction of forward scattered light, i.e.,

$$F = (1/2) \int_0^{\pi/2} x(\beta) \sin \beta \, d\beta, \quad (2.7)$$

a is the fraction of light scattered by the coarse fraction

$$a = \frac{C_c \sigma_c^0}{C_c \sigma_c^0 + C_f \sigma_f^0} = \frac{\sigma_c^0 C_c / C_f}{\sigma_c^0 C_c / C_f + \sigma_f^0}. \quad (2.8)$$

One of the basic integral parameters of the scattering phase function is the mean square of the deflection angle in the scattering event at $0 \leq \beta \leq \pi/2$, i.e., the quantity

$$\beta_2 = \int_0^\pi x(\beta) \beta^2 \sin \beta \, d\beta / \int_0^\pi x(\beta) \sin \beta \, d\beta. \quad (2.9)$$

On the basis of the data presented in Ref. 13, for the scattering phase functions of coarse ($x_c(\beta)$) and fine ($x_f(\beta)$) fractions we have

$$\beta_{2c} \approx 3.45 \cdot 10^{-3}, \quad \beta_{2f} \approx 0.27. \quad (2.10)$$

Correspondingly, the parameter β_2 for the scattering phase function given by Eq. (2.6) is

$$\beta_2 = a\beta_{2c} + (1 - a)\beta_{2f}. \quad (2.11)$$

Processing of a large sample of experimental scattering phase functions of sea and ocean water has shown that between β_2 and F the following correlation dependence exists:

$$1 - F \approx \beta_2/3. \quad (2.12)$$

The accuracy of relation (2.12) is illustrated by Fig. 1 showing the data of numerical processing of the scattering phase functions.

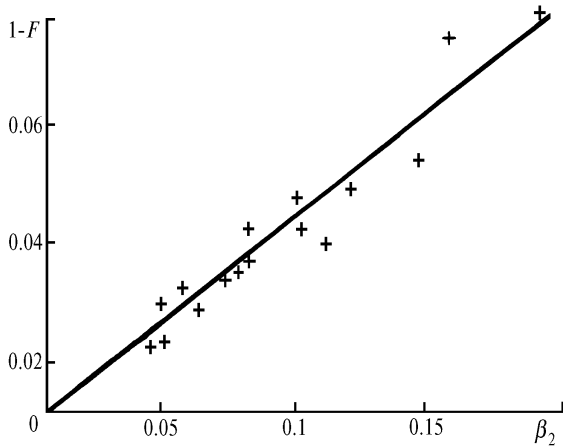


FIG. 1. Dependence of the quantity $1-F$ on the parameter β_2 .

Thus, we have obtained the single-parameter model describing the scattering phase function of the sea. The single parameter appearing in it is the quantity a , i.e., the fraction of light scattered by the coarse fraction. It may be determined, for example, by specifying C_c/C_f . The parameter a is used for determining the integral parameters of the scattering phase function β_2 and F based on Eqs. (2.11) and (2.12). Variation of a , i.e., of the ratio between the concentrations of the suspension fractions C_c/C_f , permits us to outline the variability of the scattering phase functions for different regions of the global ocean.

Moreover, the completely analytical single-parameter description of the total scattering phase function can be employed. Within the interval $[0, \pi/2]$ the functions $x_c(\beta)$ and $x_f(\beta)$ can be quite exactly and simply approximated by the formulas:

$$x_c(\beta) = 2b_c^2 \exp(-b_c\beta), \quad x_f(\beta) = 2b_f^2 \exp(-b_f\beta) \quad (2.13)$$

with

$$b_c = 41.7 \text{ rad}^{-1}, \quad b_f = 4.6 \text{ rad}^{-1}. \quad (2.14)$$

The initial¹³ and approximated data are compared in Fig. 2. Note that if $x_i(\beta) = 2b_i^2 \exp(-b_i\beta)$ then $\beta_{2i} = 6/b_i^2$.

On account of Eq. (2.13) formula (2.6) takes the form

$$x(\beta) = \begin{cases} 2F[ab_c^2 \exp(-b_c\beta) + (1-a)b_f^2 \exp(-b_f\beta)], & 0 \leq \beta \leq \pi/2, \\ 2(1-F), & \pi/2 \leq \beta \leq \pi. \end{cases} \quad (2.15)$$

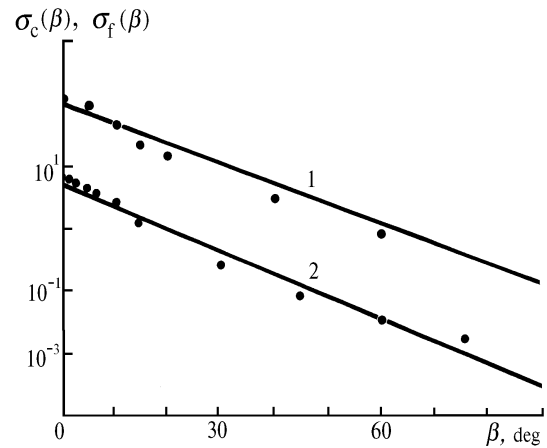


FIG. 2. Scattering phase functions of coarse $\sigma_c(\beta) = \sigma_c^0 x_c(\beta)$ (curve 1, scale is indicated above the x axis) and fine $\sigma_f(\beta) = \sigma_f^0 x_f(\beta)$ (curve 2) fractions of hydrosol according to the data of Ref. 13 (dots) and their fitting with the use of formulas (2.13) and (2.14) (straight lines).

The data available permit us to expect the significant correlation of the parameter a with the extinction coefficient ϵ . This makes it possible to relate each value of ϵ to the scattering phase function. However, as can be judged from the experimental data of Refs. 13 and 14, such correlations have the regional character.

Analysis of the available experimental data on the scattering phase functions typical of different water areas of the global ocean allows us to conclude that the scattering phase functions typical of pure ocean water are comparatively slightly variable. The same case also occurs for more turbid sea water. The most typical a values are 0.69 for ocean water and 0.62 for sea water. For this reason, some typical models of the "sea" and "ocean" phase functions can be employed for prognostic and methodical calculations. The parameters of these models are listed in Table II.

TABLE II. The parameters of the model scattering phase functions.

Water type	Parameters			Comment
	α	β_2	$1 - F$	
Ocean	0.69	0.086	0.029	$\beta_{21} = 3.45 \cdot 10^{-3}$
Sea	0.62	0.105	0.035	$\beta_{21} = 0.27$

Photon survival probability. Measurement of the photon survival probability Λ is the most complicated methodical and technical problem. For this reason it is especially important that in the physical model of the optical properties of the sea water the quantities Λ and ϵ are related in a simple way.

The extinction coefficient of sea water represents the additive sum of the extinction coefficients of all optically active components of sea water

$$\epsilon = \epsilon_{\text{sus}} + \kappa_y + \epsilon_w, \quad (2.16)$$

where ϵ_{sus} and ϵ_{w} are the extinction coefficients of suspension and water, respectively, κ_{y} is the absorption coefficient of the dissolved yellow matter. In the atmospheric transparency window (at $\lambda \approx 550$ nm) the absorption by suspension can be neglected ($\sigma_{\text{sus}} = \epsilon_{\text{sus}}$). Then, taking into account the fact that $\epsilon_{\text{w}} = \kappa_{\text{w}} + \sigma_{\text{w}}$ and $\sigma = \sigma_{\text{sus}} + \sigma_{\text{w}}$, we have

$$\epsilon = \sigma + \kappa_{\text{y}} + \kappa_{\text{w}}. \tag{2.17}$$

At $\lambda = 550$ nm the absorption by the yellow matter is negligible. In accordance with Ref. 14, for different water areas of the global ocean $\kappa_{\text{y}}/\epsilon \approx 0.02-0.07$. We introduce a small correction for the absorption by yellow matter using its mean value $\kappa_{\text{y}}/\epsilon = 0.045$. Then, taking into account that $\kappa_{\text{w}} \approx 0.035 \text{ m}^{-1}$, for the quantity $1 - \Lambda = \kappa/\epsilon$ we have

$$1 - \Lambda = 0.045 + 0.035/\epsilon, \tag{2.18}$$

i.e., we finally obtain

$$\Lambda = 0.955 - 0.035/\epsilon. \tag{2.19}$$

Relation (2.19) was obtained previously in Ref. 15 where its high accuracy within the interval $0.1 \text{ m}^{-1} < \epsilon < 0.5 \text{ m}^{-1}$ was demonstrated for different water areas of the global ocean (see Fig. 3).

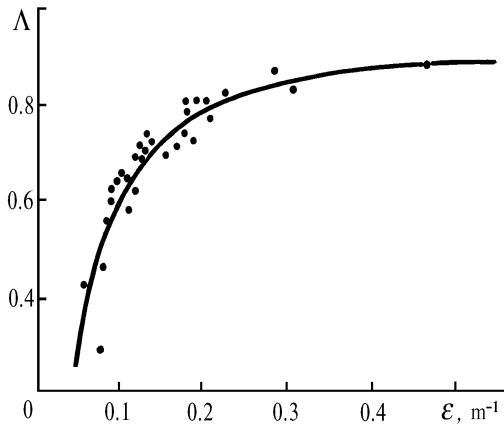


FIG. 3. Correlation between the parameters Λ and ϵ . The curve is plotted with the use of formula (2.19), the experimental results obtained in Refs. 13–16 for different regions of the global ocean are shown by dots.

Thus, the following few-parameter correlation model can be used in calculations. The type of water is specified and the value of ϵ is assigned. The type of water (sea water or ocean water) determines the scattering phase function (see Table II and formula (2.15)), while the quantity ϵ determines Λ based on relation (2.10).

The developed program implies another possibility, that is, assigning the values of ϵ , Λ , and the characteristics of the scattering phase function (a , β_1 , and β_2) at the user's discretion. This may be useful, for example, in the case in which more adequate regional characteristics of sea water are well known (especially when they are anomalous), as well as in the analysis of the sensitivity of the visibility range to the variation (or to the accuracy of assigning) of the hydrooptical characteristics.

We note that in order to modify the elongation of the scattering phase function it is sufficient to vary only the quantity a . When assigning the parameters of the experimental phase function it is necessary to keep in mind that β_{21} is the mean square of the scattering angle averaged over certain small-angle part of the scattering phase function, β_{22} is that averaged over the rest part of the scattering phase function in the interval $[0, \pi/2]$, and a is the fraction of the scattered light corresponding to the small-angle part of the scattering phase function. The division of the scattering phase function into two parts, generally speaking, is arbitrary. The division for which $a \approx 0.4-0.7$ may be recommended. In addition, the experience of processing of the marine scattering phase functions has shown that in the interval $[0, \pi/2]$ they are fitted sufficiently well by the sum of two exponentials

$$x(\beta) = B_1 \exp(-b_1 \beta) + B_2 \exp(-b_2 \beta). \tag{2.20}$$

In this case

$$\beta_{21} = 6/b_1^2, \quad \beta_{22} = 6/b_2^2, \quad a = B_1/2b_1^2.$$

Wavy sea surface. We will consider the typical states of the sea surface, that is, the wind-driven sea waves, swell, and combined waves in which the maxima of spatial energy spectra of the wind-driven waves $A_1^2(\mathbf{v})$ and the swell $A_2^2(\mathbf{v})$ are spaced. In this case the spatial spectrum of the interface can be represented in the form¹⁷

$$A_0^2(\mathbf{v}) = A_1^2(\mathbf{v}) + A_2^2(\mathbf{v}). \tag{2.21}$$

For simplicity we assume that both waves propagate along the same direction (along the direction of the object critical size). They are described by one-dimensional spectra and, in addition, the dispersive relation holds for the gravitational surface waves.

We will take the Pearson–Moscovits modified spectrum of the wind-driven waves proposed in Refs. 18 and 19

$$A_1^2(\mathbf{v}) = \frac{a_1}{v^4} \exp\left(-\frac{z_1}{v^2} - \beta_1 v^2\right) \delta(\varphi - \varphi_0), \tag{2.22}$$

where a_1 is the constant for the Pearson–Moskovits spectrum ($a_1 = 0.00405$), $z_1 = 0.74 g^2/V^4$, g is the acceleration of gravity, V is the wind speed, φ is the azimuthal angle in the plane of the interface, φ_0 characterizes the direction of wave propagation, $\beta_1 = \beta_1(V)$ is the parameter adjusted in such a way that the dependence of the variance of the wind-driven sea waves on the wind speed follows the Cox–Munk data.²⁰

We choose the swell spectrum from the following considerations. It is well known that after the termination of the wind only the region of the principal maximum, which can be described quite acceptably by the relations of the linear hydrodynamic model of the sea surface, remains in the wave spectrum. On account of this fact as well as the dispersive relation¹⁷ for swell we can write down

$$A_2^2(\mathbf{v}) = \frac{a_2}{v^4} \exp\left(-\frac{z_2}{v^2} - \beta_2 v^2\right) \delta(\varphi - \varphi_0), \tag{2.23}$$

where $a_2 = 217 h_3^2/(g\tau_3^2)$, h_3 and τ_3 are the mean height and the mean period of the swell waves (the parameters that

are normally determined when viewing the wind-driven waves), and $z_2 = 683/(g\tau_3^2)^2$. Here we introduce the parameter $\beta_2 = 1/v_1^2$ which is responsible for decreasing the spectral density beyond the region of the principal maximum, where v_1 specifies the lower boundary of the transit interval of the spectrum ($v_1 \approx 91/(g\tau_3^2)$).

2.2. The atmosphere. The atmospheric model is based on the Standard Radiative Atmosphere Model adopted by the International Commission on Radiation.^{21,22} In accordance with Refs. 21 and 22 we prescribe the molecular atmosphere as well as the types, optical constants, microstructure, and vertical stratification of aerosols. The lower atmospheric layers experience the maximum variability and play the dominant role in attenuating and scattering of radiation. For this reason in the atmospheric model the layers above 6 km are considered as one layer with the mean optical characteristics. The scattering phase functions and the extinction coefficients of the atmospheric aerosols were calculated from the Mie formulas on the basis of the data on microstructure and optical constants given in Refs. 21 and 22. The characteristics of the atmospheric models are listed in Table III. Here τ^m is the optical thickness of the corresponding atmospheric layer due to molecular scattering with the Rayleigh scattering phase function $x(\beta) = 0.75(1 + \cos^2\beta)$ at $\lambda = 550$ nm, β is the scattering angle, and τ^a is the aerosol optical thickness of stratum also at $\lambda = 550$ nm, which is determined by the composition and particle number density of aerosol. In accordance with Ref. 23 we assume that in the lower atmospheric layer adjacent to water the aerosol number density decreases exponentially with increase of the altitude, i.e., the aerosol extinction coefficient at the altitude H for $H < 2$ km is equal to

$$\epsilon_a = \frac{3.55}{S_m} \exp(-\alpha H), \tag{2.24}$$

where $\alpha = 0.92$ (from Ref. 24), S_m is the meteorological visibility range (MVR, km) and characterizes the optical conditions in the atmosphere in the layer adjacent to water at the moment of observation of the object.

TABLE III. Atmospheric model.

Altitude above the sea level H , km	Serial number of the layer	Aerosol type	τ^m	τ^a
0–2	1	Marine	0.021	$3.246/S_m$
2–6	2	Continental	0.031	0.020
$H > 6$	3	Continental $H < 20$ km Stratospheric $H > 20$ km	0.046	0.019

Thus, the only adjustable parameter in the atmospheric model is the quantity MVR. In so doing the aerosol optical thickness of lower 2–km layer adjacent to water at $\lambda = 550$ nm is

$$\tau_1^a = 3.246/S_m. \tag{2.25}$$

The phase functions of light scattering by the atmospheric aerosols are approximated as follows:

$$x_a(\beta) = \sum_{i=1}^2 B_i \exp(-b_i\beta) + \tilde{x}_a(\beta), \tag{2.26}$$

where the exponential terms describe the aureole part of the scattering phase function and $x_a(\beta)$ is a slowly varying function. The light fraction F_β^a associated with the aureole part of the scattering phase function and scattered at the angles $[0, \beta]$ is given by the formula

$$F_\beta^a = \sum_i \frac{B_i}{2b_i^2} [1 - (b_i\beta + 1) \exp(-b_i\beta)]. \tag{2.27}$$

The parameters used in calculations of the scattering phase functions are given in Table IV for two main types of atmospheric aerosols: marine and continental. In addition to B_i , b_i , and F_β^a ($\beta = 20$), the values of the aerosol phase functions at the angle $\beta = \pi/2$ are also listed in the table. Stratospheric aerosol has practically no effect on the calculated quantities, and its parameters are omitted.

TABLE IV. Parameters of the scattering phase functions of atmospheric aerosols.

Aerosol type	Parameters				$\tilde{x}_a(\beta)$		F_β^a	
	B_1	B_2	b_1	b_2	$\beta = \pi/2$	$\beta = \pi$	$\beta = 20^\circ$	$\beta = 90^\circ$
Marine	630	30.0	40	5.3	0.16	0.60	0.427	0.895
Continental	602	16.7	90	3.3	0.30	0.37	0.281	0.885

We note that the above-described atmospheric model is one of the simplest models. It is especially useful in prognostic investigations. If necessary, the regional and special local optical models can be employed in the program, which are formed on the basis of the databank and the procedures of the ATMOTOOLS package.²⁵

3. THE PARAMETERS OF THE VIEWING SYSTEM

Let us consider the basic parameters of the system which determine the visibility range. For simplicity we divide all the parameters into eight groups referred to as System, Geometry, Source, Detector, Medium, Object, Illumination, and Backscatter interference.

System. This method is intended to assess the limiting possibilities of passive (when the object is illuminated by the sun) and active laser–television viewing systems. In so doing it is assumed that the active system can operate both at night and in the daytime.

The reliability of detection (discrimination) is specified by the erroneous alarm probability P_{er} and detection probability P_{det} , which in accordance with the system of equations (1.8) and relation (1.9) determine the threshold signal–to–noise ratio.

Geometry. It is assumed that the television system is located underwater or is placed onboard the aircraft located at the altitude H above the sea level and observations are performed at the angle $\theta_0 = \arccos \mu_0$ with respect to the vertical, which corresponds to the angle $\theta'_0 = \arccos \mu'_0$ after refraction of a ray in water. The case $H = 0$ corresponds to the underwater television system.

Source. It is assumed that in the active system the laser source is used (operating in a pulsed or continuous regime), its divergence $2\gamma_s$ determines the illuminated spot size on the ocean surface $R_s = 2\gamma_s H/\mu_0$. In so doing it is assumed that in the cases of $H > 0$ and $H = 0$ (underwater variant) the beam divergence in the water is $2\gamma'_s = 2\gamma_s/n$ (in the underwater variant the beam enters the water through a porthole).

For a pulsed source with the pulse energy W_0 and the number of pulses N_p the total energy emitted by the source over the period of frame recording is $W = W_0 N_p$. For a stationary source by the quantity $W = W_0 N_p$ we understand the radiation source energy emitted over the period of frame recording.

Detector. It is assumed that the television tube with the number of lines M and threshold contrast k_{th} is a detector. The quantity k_{th} being measured in practice specifies the parameter α of the video system intrinsic noise based on relation (2.7). The characteristic of the photodetector is also the constant

$$C = S_k T_{opt} A / e(1 + B),$$

where S_k is the spectral sensitivity of the photocathode, T_{opt} is the efficiency of the optical system, e is the electron charge, B is the gain of fluctuation noise caused by the secondary emission, and A is certain coefficient (for a superorthicon $A \approx 0.3$ according to Refs. 24 and 26). For $S_k = 0.05$ A/W, $T_{opt} = 0.5$, $B = 1$, and $A = 0.3$ the quantity $C = 2.34 \cdot 10^{16}$ J⁻¹. As has already been noted, the constant C is related to the photodetector quantum efficiency η . At $\lambda = 500$ nm the quantity $C = 2.34 \cdot 10^{16}$ J⁻¹ corresponds to $\eta \approx 0.01$.

The diameter of input pupil of the photodetector is equal to D_{det} . The aperture angle of the detector field of view $2\gamma_{det}$ determines the frame size. The frame size at the ocean surface is equal to $2\gamma_{det} H / \mu_0$. It is assumed that the viewing system refers to the "broad-narrow" type, i.e., the entire frame is illuminated ($2\gamma_s \geq 2\gamma_{det}$).

Medium. The adopted models of the sea and atmosphere have been described in Sec. 2. In addition, the following possibilities are provided with the algorithmic implementation of the program. The parameters typical of ocean and sea scattering phase functions, which have been presented in Sec. 2.1, are entered in the program. The user must only choose the water type. For the experimental scattering phase function it is necessary to assign the parameters α , β_{21} , and β_{22} . In addition, the extinction coefficient ε is assigned. The quantity Λ either is assumed to be correlated Λ_{cor} (in this case it is given by formula (3.19)) or may be taken from experiment.

Thus, when we construct the model of the sea using Λ_{cor} , we must only choose the water type and assign ε .

Another limiting variant is possible, in which ε , λ , and the parameters of the scattering phase function (which is taken from the experiment) are assigned independently. Also, the combined variants can be realized (for example, Λ_{cor} is used while the phase function is taken from experiment or the water type and the value of ε are assigned while Λ is taken from experiment).

In order to describe the state of the atmosphere-water interface, its type is chosen (smooth or wavy surface). For wavy surface the wind speed V and the mean height h_3 and the mean period τ_3 of swell waves are assigned.

The model and parameters of the atmosphere are presented in Sec. 2.2. Here the only variable parameter assigned in the model is the meteorological visibility range S_m (in kilometers) at the sea level.

Object. The observed object is located at the depth L and characterized by the smallest (critical) size d_{xob} and by the size d_{yob} in the perpendicular direction. It is assumed

that the object reflects according to the Lambert law and possesses the albedo A_{ob} .

Illumination. In the study of the passive and active systems operating during the day, the background illumination caused by the solar radiation reflected and scattered by the sky, sea, and interface is taken into account. The elevation of the sun above the horizon is characterized by the angle $\theta_s = 90^\circ - \arccos \mu_s$. The illumination intensity is proportional to the period of frame recording t_f and to the bandwidth of the filter $\Delta\lambda$ of the detector.

Backscatter interference. In the study of the active viewing systems it is necessary to calculate the power of the backscatter interference (BSI). Two sources of the BSI are taken into account: the first is associated with backscattering of laser radiation in water, while the second – with backscattering in the atmosphere.

The power of the BSI recorded by the photodetector is a function of the following parameters of the system: L_1 , i.e., the start of the spatial gating of the BSI with depth (the value of L_1 is counted off from the object) and Δt_{str} is the duration of temporal strobe.

4. CALCULATIONAL FORMULAS

In order to calculate the maximum ranges of detection and discrimination of the object in the scattering medium it is necessary to solve Eqs. (1.16) and (1.18) on account of Eq. (1.11). In so doing it is necessary to know the calculational formulas for the function ψ_1 as well as for the energies of the valid signal W_{vs} and background W_{bg} . For brevity we restrict ourselves mainly to the structural formulas interpreting only their principal terms.

4.1. Energy of the background. The portion of the background caused by scattering and reflection of solar radiation we will call the illumination. An account of the illuminations is necessary when calculating the visibility range for passive systems and for active systems operating during the day. Another portion of the background, i.e., the backscatter interference (BSI), is caused by the radiation emitted by the illumination source and scattered by the medium (by water and atmosphere). Its contribution is important for evaluating the possibilities of the active systems.

Illumination. The energy of the solar illumination at the input of the photodetector is

$$W_{il} = W'_{il} d_{xel}^{opt} d_{yel}^{opt}, \quad (4.1)$$

where d_{xel}^{opt} and d_{yel}^{opt} are determined by solving the system of equations (1.16) in the problem of detection of the object and are given by Eq. (1.17) in the case of discrimination of the object. The energy density of illuminations calculated per unit area of the object is

$$W'_{il} = I \Sigma_{det} t_f \Delta\lambda / z^2, \quad (4.2)$$

where I is the intensity of solar illuminations at the input of the photodetector, $\Sigma_{det} = \pi D_{det}^2 / 4$ is the area of the input pupil of the photodetector, D_{det} is the diameter of the input pupil, t_f is the period of frame recording (in the case of active viewing system $t_f = \Delta t_{str} N_f$), $\Delta\lambda$ is the filter bandwidth, the quantity

$$z = H / \mu_0 + L / n\mu'_0 \quad (4.3)$$

determines the solid receiving angle, which is equal to $d_{x\text{el}}^{\text{opt}} d_{y\text{el}}^{\text{opt}} / z^2$,

$$\mu'_0 = \sqrt{(\mu_0^2 + n^2 - 1)/n^2} \tag{4.4}$$

is the cosine of the viewing angle in water on account of refraction. Formula (4.3) takes into account the change of the solid angle when passing through the air – water interface.

The intensity of solar illuminations at the input of the photodetector represents the sum of four basic components

$$I = (E_s \mu_s / \pi) [\rho_a(H) + \rho_{wd} + \rho_{dif}^m + \rho_{dif}^{int}] , \tag{4.5}$$

where $E_s = 2 \text{ J/m}^2\text{-nm}\cdot\text{s}$ is the solar constant, i.e., the solar illumination of the area oriented normally and placed at the upper boundary of the atmosphere in the unit wavelength interval centered at $\lambda = 550 \text{ nm}$; $\rho_a(H)$ is the brightness coefficient (BC) of light reflected by the atmospheric layer of the thickness H adjacent to water on account of the extinction of the solar radiation by the upper atmospheric layer H^* ; ρ_{wd} is the BC of light reflected by the sea water illuminated by the directional light (direct solar radiation and aureole part of scattering in the atmosphere) on account of atmospheric extinction of the incident light and light scattered by the sea; ρ_{dif}^m and ρ_{dif}^{int} are the BC's of the light reflected by sea water and surface illuminated by scattered sky light taking into account its extinction on the path to the radiation detector.

The specular reflection of directional radiation by the sea surface is neglected here because the detuning from the sun's glitter pattern is performed.

The brightness coefficients entering into formula (4.5) can be calculated with the help of the quasi-single-scattering approximation. In particular,

$$\rho_a(H) = \frac{x_a(\cos\beta)}{4(1 - F_H)(\mu_s + \mu_0)} \times \left\{ 1 - \exp\left[-\tau_H(1 - F_H)\left(\frac{1}{\mu_0} + \frac{1}{\mu_s}\right)\right] \right\} \exp\left[-\tau_H^*(1 - F_H^*)/\mu_s\right], \tag{4.6}$$

where τ_H and F_H are the optical thickness and the fraction of light scattered forward in the elementary volume as applied to the atmospheric layer (0, H); τ_H^* and F_H^* are the total optical thickness of the atmosphere without the lower layer of thickness H and the fraction of light scattered forward in this region of the atmosphere;

$$\rho_{wd} = \frac{\Lambda(1 - F)}{2n^2(1 - \Lambda F)(\mu'_0 + \mu'_s)} T_{atm}^{pas} T_{int}(\mu_0) T_{int}(\mu_s) , \tag{4.7}$$

n is the water refractive index; $T_{int}(\mu)$ is the transmission of the water–air interface, T_{atm}^{pas} is the transmission of direct light and the aureole fraction of light scattered by the atmosphere.

Backscatter interference. In analogy with Eq. (4.1) we write down the energy of the BSI in the form

$$W_{bs} = W'_{bs} d_{x\text{el}}^{\text{opt}} d_{y\text{el}}^{\text{opt}} . \tag{4.8}$$

The BSI is caused by scattering of radiation in water ($W'_{bs\text{w}}$) and in the atmosphere ($W'_{bs\text{a}}$), i.e.,

$$W'_{bs} = W'_{bs\text{w}} + W'_{bs\text{a}} . \tag{4.9}$$

It is assumed that for a pulsed laser source the partial temporal cutoff of the BSI can be performed. In so doing the strobe of duration Δt_{str} switches on the detector of radiation at the moment of the signal arrival from the point located at the distance L_1 from the object. Thus, the detector receives the radiation backscattered by the layer of the medium extending from $L - L_1$ to $L - L_1 + c\Delta t_{str}/2n$ (c/n is the velocity of light in the medium). Then

$$W'_{bs\text{w}} = \frac{W_0 N_p}{\pi n^2} \frac{\Sigma_{det}}{(2\gamma_s)^2 z^2} \rho_w(L_1, \Delta t_{str}) T_{int}^2(\mu_0) , \tag{4.10}$$

where $W_0 N_p$ is the total energy of the source emitted over the period of frame recording t_f , the quantity z is given by formula (4.3), and $\rho_w(L_1, \Delta t_{str})$ is the brightness coefficient in the backward direction of the sea water layer engendering the BSI.

The power $W'_{bs\text{a}}$ is formed as follows. The laser beam undergoes reflection from the sea surface, backscattering in the atmosphere, and one more specular reflection from the sea surface and enters the detector, i.e.,

$$W'_{bs\text{a}} = \frac{W_0 N_p}{\pi} \frac{\Sigma_{det}}{(2\gamma_s)^2 z^2 z_1^2} \rho_a(L_1, \Delta t_{str}) R_{int}^2(\mu_0) . \tag{4.11}$$

Here $R_{int}(\mu_0)$ is the coefficient of specular reflection by the sea surface when light is incident on it at the angle $\arccos \mu_0$, $z_1 = H/\mu_0 + L_1 n/\mu'_0$, and $\rho_a(L_1, \Delta t_{str})$ is the brightness coefficient of the atmospheric layer of thickness $c\Delta t_{str}/2$ adjacent to the water surface in the backward direction.

4.2. Energy of the valid signal and the function Ψ_1 .

Detection. In accordance with Eqs. (1.14) and (1.15) the relation for the valid signal energy W_{vs} has the form

$$W_{vs} = W \eta_{vs} |A_{ob} - A_{bg}| \Psi_1 , \tag{4.12}$$

$$\eta_{vs} = \eta'_{vs} d_{x\text{el}}^{\text{opt}} d_{y\text{el}}^{\text{opt}} . \tag{4.13}$$

For the passive viewing system (illuminated by the sun) it is necessary to set

$$W = E_s t_f \Delta \lambda , \tag{4.14}$$

$$\eta'_{vs} = \frac{\mu_s}{\pi n^2} \frac{\Sigma_{det}}{z^2} T_{atm}^{pas} \exp\left\{- (1 - \Lambda F) \varepsilon L \left(\frac{1}{\mu'_s} + \frac{1}{\mu'_0}\right)\right\} , \tag{4.15}$$

$$A_{bg} = \frac{\Lambda(1 - F)}{4(1 - \Lambda F)} . \tag{4.16}$$

For the active viewing system

$$W = W_0 N_p , \tag{4.17}$$

$$\eta'_{vs} = \frac{1}{\pi n^2} \frac{\Sigma_{det}}{(2\gamma_s)^2 z^4} T_{atm}^{act} \exp[-2(1 - F) \varepsilon L/\mu'_0] , \tag{4.18}$$

where

$$T_{\text{atm}}^{\text{act}} = \exp[-2(1 - F_H) \tau_H / \mu_0], \quad (4.19)$$

$$A_{\text{bg}} = \frac{\Lambda(1 - F)}{4(1 - \Lambda F)} \left\{ 1 - \exp \left[-(1 - \Lambda F) e \left(\frac{c\Delta t_{\text{str}}}{n} - \frac{2L_1}{\mu'_0} \right) \right] \right\}. \quad (4.20)$$

The relation for the function ψ_1 in the general case has the form⁴

$$\Psi_1 = \frac{1}{4\pi^2 \langle A_{\text{ob}} \rangle} \int_{-\infty}^{\infty} \int_{-\infty}^{\infty} A_{\text{ob}}(\mathbf{v}) T(\mathbf{v}) U(\mathbf{v}, \Sigma_{\text{el}}) d\mathbf{v}. \quad (4.21)$$

Here $A_{\text{ob}}(\mathbf{v})$ and $U(\mathbf{v}, \Sigma_{\text{el}})$ are the Fourier spectra (\mathbf{v} is the spatial frequency) of the spatial distribution of object albedo $A_{\text{ob}}(\mathbf{r})$ and of the function

$$U(\mathbf{r}, \Sigma_{\text{el}}) = \begin{cases} 1, & \text{for } \mathbf{r} \in \Sigma_{\text{el}} \\ 0, & \text{for } \mathbf{r} \notin \Sigma_{\text{el}}, \end{cases}$$

respectively, $T(\mathbf{v})$ is the frequency-contrast characteristic (FCC) of the medium allowing for blurring of the image due to scattering of light in the medium on the observation path, and $\langle A_{\text{ob}} \rangle$ is the mean albedo of the object. For the uniform object of rectangular shape we have

$$\Psi_1 = \Psi(d_{x \text{ ob}}/2, d_{y \text{ ob}}, d_{x \text{ el}}, d_{y \text{ el}}), \quad (4.22)$$

where

$$\begin{aligned} \Psi(d_{x \text{ ob}}, d_{y \text{ ob}}, d_{x \text{ el}}, d_{y \text{ el}}) &= \frac{1}{4\pi^2} \int_{-\infty}^{\infty} \int_{-\infty}^{\infty} \frac{\sin(v_x d_{x \text{ ob}}/2) \sin(v_y d_{y \text{ ob}}/2)}{v_x/2} \times \\ &\times T\left(\sqrt{v_x^2 + v_y^2}\right) \frac{\sin(v_x d_{x \text{ el}}/2)}{v_x d_{x \text{ el}}/2} \frac{\sin(v_y d_{y \text{ el}}/2)}{v_y d_{y \text{ el}}/2} dv_x dv_y. \end{aligned} \quad (4.23)$$

We stress that in formula (4.22) $d_{x \text{ ob}}$ and $d_{y \text{ ob}}$ are the dimensions of the real object along the critical x axis and along the y axis. In representation (4.22) the fact that the size of Jonson's test object along the x axis is equal to half the size of the real object in the problem of object detection is taken into account.

In order to calculate the FCC of the water layer, the small-angle approximation of the transfer theory can be used. By fitting the scattering phase function by the sum of two exponentials we have¹

$$\begin{aligned} T(\mathbf{v}) &= \exp \left\{ -\frac{\Lambda \epsilon L}{\mu'_0} \left[1 - a \left[1 + \frac{\beta_{21}}{6} \left(\frac{vL}{\mu'_0} \right)^2 \right]^{-1/2} - \right. \right. \\ &\left. \left. - (1 - a) \left[1 + \frac{\beta_{22}}{6} \left(\frac{vL}{\mu'_0} \right)^2 \right]^{-1/2} \right] \right\}. \end{aligned} \quad (4.24)$$

Relations (4.21)–(4.24) determine the function ψ_1 .

Discrimination. In the problem of object discrimination in accordance with Jonson's criteria the eight half-periods of the hatched mira must be resolved on the object of critical size. For this reason in formula (1.11) for

signal-to-noise ratio δ the quantity W_{vs} is the difference between the energy acquired by the light element of the area $\Sigma_{\text{el}}^{\text{opt}}$ (see formula (1.17)) and the mean energy W_{bg} acquired by the same area of the object image. Replacing approximately the hatched mira by the sinusoidal one and making allowance for the boundness of the object by the method proposed in Ref. 2 we have

$$W_{\text{vs}} = W \eta_{\text{vs}} \frac{|A_{\text{ob}} - A_{\text{bg}}|}{2} T(\mathbf{v}), \quad (4.25)$$

where η_{vs} , $T(\mathbf{v})$, and A_{bg} are given by formulas (4.17), (4.19), (4.15), and (4.24), respectively. In calculation of $T(\mathbf{v})$ the frequency of the equivalent eight half-period mira is

$$v = 8\pi/d_{x \text{ ob}}. \quad (4.26)$$

In this case the relation for the mean energy W_{bg} of the object image has the form

$$W_{\text{bg}} = W_{\text{bg}}' d_{x \text{ el}}^{\text{opt}} d_{y \text{ el}}^{\text{opt}}, \quad (4.27)$$

where

$$W_{\text{bg}}' = W_{\text{il}}' + W_{\text{bs}}' W \eta_{\text{vs}}' \frac{|A_{\text{ob}} - A_{\text{bg}}|}{2} \Psi(d_{x \text{ ob}}, d_{y \text{ ob}}, d_{x \text{ el}}^{\text{opt}}, d_{y \text{ el}}^{\text{opt}}), \quad (4.28)$$

$d_{x \text{ el}}^{\text{opt}}$ and $d_{y \text{ el}}^{\text{opt}}$ are given by formula (1.17)

5. SOME EXAMPLES OF THE APPLICATION OF THE METHOD

The elaborated theory includes, as particular cases, the well-known results of vision theory and, in addition, gives their natural generalization. As an illustration we will consider two classic examples, that is, Coshmider's theory of horizontal visibility in the atmosphere and the depth of visibility of the Secchi disk in the sea water.

Horizontal visibility range. When observing under conditions of solar illumination it can be assumed that $\alpha C W_{\text{bg}} \gg 1$ in Eq. (1.11). Then the limitations on the visibility range are imposed by the vanishing contrast. If the object is small enough and its albedo $A_{\text{ob}} = 0$ then, as it has been shown in Ref. 4, the use of the above-described method yields the well-known formula for the horizontal meteorological visibility range (MVR) of the object

$$S_{\text{m}} = -(\ln k_{\text{th}}) / \epsilon. \quad (5.1)$$

For the threshold contrast of vision $k_{\text{th}} = 0.02$ the quantity S_{m} is equal to $3.91/\epsilon$.

However, the possibilities of the given method are wider than derivation of relation (5.1). It can be used to evaluate in practice the requirement of Coshmider's theory for the object to be small. Figure 4 shows the dependence of ϵL^* (L^* is the visibility range) on the optical size ϵd of the square object with side d and albedo $A_{\text{ob}} = 0$. The dependence is obtained for a cloud with the scattering phase function calculated for C1 cloud with different values of k_{th} . As $d \rightarrow 0$ the quantity $L^* \rightarrow S_{\text{m}}$. It can be seen that the requirement for the object to be small is satisfied practically always when $d/L^* \leq 0.03$ – 0.05 , i.e., when the visible angular size of the object is less than 2° .

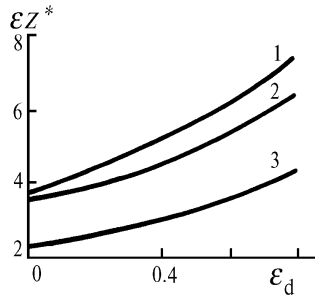


FIG. 4. The visibility range of the black object ($A_{ob} = 0$) as a function of its size for the threshold contrast $k_{th} = 0.02$ (1), 0.03 (2), and 0.1 (3).

Depth of visibility of the Secchi disk. The problem on the depth of visibility of a white disk (the Secchi disk) thrown overboard is of special interest in hydrooptics. This is connected with the estimate of the sea water transparency from the visibility depth z_d of the disk. This technique has long been adopted in hydrooptics. It has been noted in a number of investigations that

$$z_d = \beta / \epsilon, \tag{5.2}$$

where β is independent of the water optical properties. However, in practice β differs significantly for various water basins, while the depth z_d depends not only on ϵ .

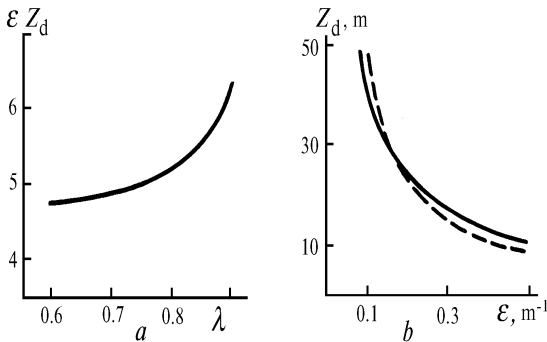


FIG. 5. Visibility of the Secchi disk. Dashed line refers to $z_d = 5/\epsilon$.

In the context of the object detection theory the quantity z_d is the maximum depth of visibility of the object of the given dimensions with fixed albedo in the case of illumination by the sun and viewing through the air–water interface. The dependences of $\beta = \epsilon z_d$ on λ as well as of the depth z_d on ϵ (for the few–parameter model of the sea water) are shown in Fig. 5. They were obtained by the method described in this paper. The calculations were performed for the standard Secchi disk 0.3 m in diameter with $A = 0.8$ for threshold contrast of vision $k_{th} = 0.03$. It can be seen that the quantity $\beta = \epsilon z_d$ grows as λ increases. The results of calculation performed with the use of the developed detection theory are in a very good agreement with the data of Ref. 27 in which the problem on the visibility of the white disk was considered in ample detail and thoroughly. The dashed line in Fig. 5b shows the dependence $z_d = 5/\epsilon$. It can be seen that for $\beta = 5$ relation (5.2) describes fairly well z_d in oceanic water, for which the few–parameter model (see Sec. 2.1) is applicable.

Viewing of the object with the help of a laser–television system. The above examples refer to the system of

passive visual observation. As an example of using the above–discussed method for estimating the systems of active viewing, Fig. 6 shows the results of calculation of the detection (solid lines) and discrimination (dashed lines) depths of the object in the oceanic water with the help of the laser–television system. It is assumed here that the object is the square with the side d , the water extinction coefficient $\epsilon = 0.1 m^{-1}$, $\lambda = 0.6$, the pulse energy $W_0 = 0.1 J$, and the object albedo $A_{ob} = 0.8$ (curves 1) and 0.2 (curves 2).

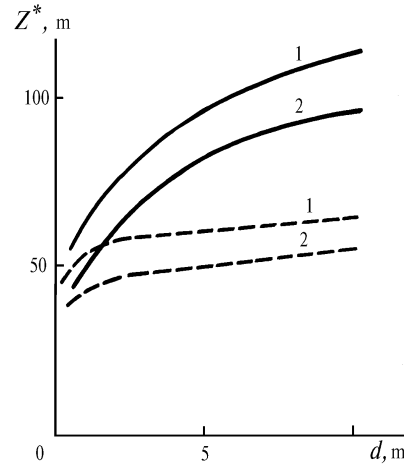


FIG. 6.

Viewing through the wavy sea surface. As the second example of estimating the systems of active viewing we consider the maximum depth of visibility when viewing the object with the help of a pulsed laser–television system through the wavy sea surface. Shown in Fig. 7 is the depth of detection of the object in the shape of a square with 1 m side as a function of the wind speed (Fig. 7a) and of the period of swell waves 1 m in height (Fig. 7b). It can be seen that for such a small object with increase of the wind speed up to 3 m/s the detection depth decreases rapidly down to some value and further remains practically constant. In some cases (curve 2 at $\epsilon = 0.4 m^{-1}$) L_{det}^* changes abruptly. Such a behavior can be explained as follows.

For wind–driven sea waves the dependence of K_f describing the contribution of noise caused by sea waves on the depth of location of the layer generating the BSI, has the distinctly pronounced maximum near the surface.¹⁸ For this reason the dependence of the signal–to–noise ratio on the depth of location of the object under the water surface disturbed by the wind–driven waves may be nonmonotonic, namely, of the form shown in Fig. 8 (the dashed lines show the dependence of the signal–to–noise ratio on the depth of the object location when viewing through the smooth interface). Such a dependence leads to a very interesting consequence. In the situation indicated by curve 2 the requirement for detectability of the object $\delta > \delta^*$ is satisfied for the depths from the surface to L_2^* , and from L_2^* , to L_2^* . This means that in the above–indicated intervals the object can be seen, while at the depths varying from L_2^* , to L_2^* it cannot be detected. It should be noted that in such a situation the notion of maximum visibility depth itself becomes not quite definite. We will refer to the limiting visibility depth L_2^* as the maximum visibility depth in spite of the fact that at certain depths $L < L_2^*$ the object is invisible. It is clear that when we go over from situation 1 to situation 3, the limiting detection depth can change abruptly.

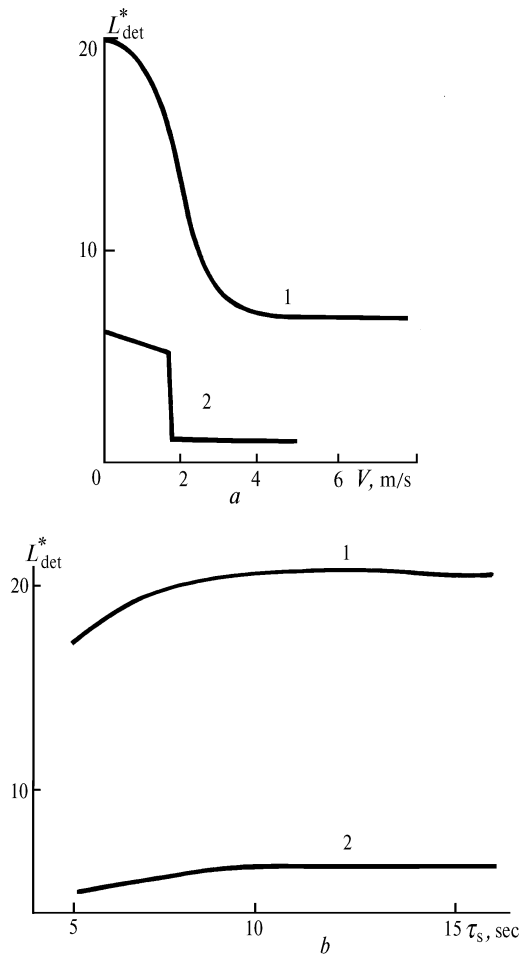


FIG. 7. Depth of detection of the 1×1 m object for observation through the wavy sea surface as a function of wind speed (a) and of the swell wave period (b) at $\epsilon = 0.1 \text{ m}^{-1}$ (1) and $\epsilon = 0.4 \text{ m}^{-1}$ (2).

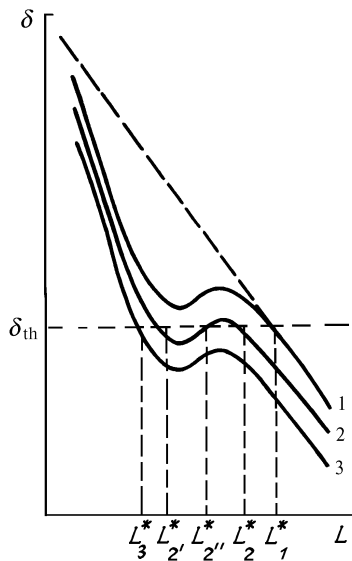


FIG. 8. Dependence of the signal-to-noise ratio on the depth of the underwater object for observation through the wavy sea surface.

The swell waves have a relatively weak effect on the detectability of the underwater object. The reason for this is the fact that the noise caused by these waves is correlated within the limits of the object image (see Sec. 1.2). Only in the case of short-period waves, whose period is comparable to the object dimensions, the surface fluctuation noise reduces the detection depth.

CONCLUSION

The developed concept of determining the object visibility range in the scattering media, which is based on the ideas of optimum processing of image, and the programs for personal computers elaborated on the basis of this concept allow one to calculate the maximum depths of detection and discrimination of underwater objects with the help of the active and passive television systems.

The criterion for optimum processing of the image is essentially similar to the well-known Neumann-Pearson criterion. The classification by the degrees of visibility is based on Jonson's criteria. The reliability of detection and discrimination is specified by the probabilities of erroneous alarm and detection, which determine the threshold value of the signal-to-noise ratio. For describing the optical properties of the ocean-atmosphere system the few-parameter models are employed.

The elaborated programs operate in the interactive mode and have the developed services (minimum requirements for the operator qualification, error diagnostics, etc.). The operator can easily and rapidly choose different geometry of observation (from the case when the viewing system is placed onboard the aircraft to the variant of underwater observation), can change the parameters of the source and detector and the characteristics of the devices for suppression of backscatter interference. This enables one to simulate the operation of almost all the possible variants of the television viewing system and to evaluate its possibilities.

The general character of the concept and the modularity of the program permit one to extend substantially its possibilities. For example, at present there exists the possibility of taking into account the polarization characteristics of signals and backgrounds in the laser-television and laser-radar systems and evaluating the efficiency of polarization discrimination of backgrounds for observations under different conditions.

REFERENCES

1. E.P. Zege, A.P. Ivanov, and I.L. Katsev, *Image Transfer Through a Scattering Medium* (Heidelberg, Springer-Verlag, 1991), 395 pp.
2. D.M. Bravo-Zhivotovskii, L.S. Dolin, A.S. Luchinin, and I.M. Levin, in: *Ocean Optics* (Nauka, Moscow, 1983), Vol. 1. pp. 9-113.
3. J. Jonson, in: *Proceedings of the Image Intensifier Symposium*, Fort Belvoir (1958).
4. I.L. Katsev and E.P. Zege, *Izv. Akad. Nauk SSSR, Fiz. Atmos. Okeana*, No. 7, 732-740 (1989).
5. A. Rouz, *Man's Sight and Electronic Imaging* [Russian translation] (Mir, Moscow, 1977), 216 pp.
6. I.L. Katsev, *Izv. Akad. Nauk SSSR, Fiz. Atmos. Okeana*, **23**, No. 1, 84-90 (1987).
7. I.L. Katsev, *Izv. Akad. Nauk SSSR, Fiz. Atmos. Okeana*, **23**, No. 1, 84-90 (1987).
8. I.L. Katsev and A.S. Prikhach, *Izv. Akad. Nauk SSSR, Fiz. Atmos. Okeana*, **26**, No. 3, 315-318 (1990).
9. Yu.P. Leonov, *Theory of Statistical Decisions and Psychophysics* (Nauka, Moscow, 1977), 288 pp.

10. M.M. Miroshnikov, *Theoretical Foundations of Opto-Electronic Devices* (Mashinostroenie, Moscow, 1983), 600 pp.
11. N.N. Krasil'nikov, *Theory of Transfer and Perception of Images* (Radio i Svyaz', Moscow, 1986), 184 pp.
12. A.A. Vas'kovskii and S.S. Romanov, *Opt. Mekh. Promst.*, No. 9, 13–16 (1987).
13. O.V. Kopelevich, "Optical properties of ocean water," Author's Abstract of Doct. Phys.-Math. Sci. Dissert., Institute of Optics of the Academy of Sciences of the USSR, Moscow (1981), 39 pp.
14. O.V. Kopelevich, in: *Ocean Optics* (Nauka, Moscow, 1983), Vol. 1. pp. 150–163.
15. A.N. Dorogin, O.V. Kopelevich, I.M. Levin, and V.I. Feigels, in: *Abstracts of Reports at the Tenth Plenum on the Optics of the Ocean*, Rostov-na-Donu (1988), pp. 136–137.
16. D.M. Phillips and J.T.O. Kirk, *Aust. J. Mar. Freshw. Res.* **35**, No. 6, 635–644 (1984).
17. I.N. Davidan, L.I. Lopatukhin, and V.A. Rozhkov, *Wind-Driven Sea Waves in the Global Ocean* (Gidrometeoizdat, Leningrad, 1985), 256 pp.
18. A.G. Luchinin and I.A. Sergievskaya, *Izv. Akad. Nauk SSSR, Fiz. Atmos. Okeana* **18**, No. 8, 850–853 (1982).
19. A.G. Luchinin and I.A. Sergievskaya, *Izv. Akad. Nauk SSSR, Fiz. Atmos. Okeana* **22**, No. 7, 773–776 (1986).
20. V.D. Pearson, in: *Wind-Driven Waves* [Russian translation] (Inostrannaya Literatura, Moscow, 1962), pp. 42–124.
21. R.A. McClathey, H.J. Bolle, and K.Ya. Kondrat'ev, *Report of the IAMAP RCWG on a Standard Radiative Atmosphere*, Preprint, Seattle, Washington (1977).
22. J. Lenoble and C. Brognier, *Beit. Phys. Atmosph.* **57**, No. 1, 1–20 (1984).
23. L. Elterman, *Appl. Optics* **9**, No. 18, 1804–1810 (1970).
24. S.B. Gurevich, *Physical Processes in Camera Tubes* (Fizmatgiz, Moscow, 1958).
25. E.P. Zege, A.S. Prikhach, and L.I. Chaikovskaya, in: *Proceedings of the Fifth International Colloquium on Physical Measurements and Signatures in Remote Sensing*, Courchevel, France (1991), pp. 13–18.
26. I.M. Levin, in: *Ocean Optics* (Nauka, Moscow, 1983), Vol. 2. pp. 187–199.
27. I.M. Levin, *Izv. Akad. Nauk SSSR, Fiz. Atmos. Okeana*, **16**, No. 9, 926–932 (1980).